On an Adaptive Coarse Space and on Nonlinear Domain Decomposition

Axel Klawonn[1], Martin Lanser[1], Patrick Radtke[1], and Oliver Rheinbach[2]

1 Introduction

We consider two different aspects of FETI-DP domain decomposition methods [8, 23]. In the first part, we describe an adaptive construction of coarse spaces from local eigenvalue problems for the solution of heterogeneous, e.g., multiscale, problems. This strategy of constructing a coarse space is implemented using a deflation approach. In the second part, we introduce new domain decomposition approaches for nonlinear problems. These methods are based on a decomposition of the nonlinear problem before linearization.

2 A Deflation Method

The coarse space of iterative substructuring methods such as FETI-DP or BDDC methods [8, 1, 23] can be enhanced by additional constraints using projections; see, e.g., [15]. The solution of a symmetric positive (semi-)definite system $F\lambda = d$ using the deflation method [19] also known as projector preconditioning [6], consists of the computation of λ from

$$M^{-1}(I-P)^T F\lambda = M^{-1}(I-P)^T d$$

by the conjugate gradient method using a projection of the form $P = U(U^T FU)^{-1}U^T F$ and a preconditioner M^{-1}. It is equivalent to solving $F\lambda = d$ by conjugate gradients using the symmetric preconditioner $M_{PP}^{-1} = (I-P)M^{-1}(I-P)^T$. With $\overline{\lambda} := PF^{-1}d$ the solution λ^* of the original problem is then computed as $\lambda^* = \overline{\lambda} + \lambda$. If we include the computation of $\overline{\lambda}$ into the iteration, we obtain the balancing preconditioner [17, 7] $M_{BP}^{-1} = (I-P)M^{-1}(I-P)^T + U(U^T FU)^{-1}U^T$. We then obtain the solution directly without an additional correction $\overline{\lambda}$.

For details on the deflation method or the balancing preconditioner applied to the FETI-DP or BDDC method, see [15].

---

[1] Mathematisches Institut, Universität zu Köln, Weyertal 86-90, 50931 Köln, Germany e-mail: {axel.klawonn}{martin.lanser}{patrick.radtke}@uni-koeln.de

[2] Institut für Numerische Mathematik und Optimierung, Fakultät für Mathematik und Informatik, Technische Universität Bergakademie Freiberg, Akademiestr. 6, 09596 Freiberg. e-mail: oliver.rheinbach@math.tu-freiberg.de

For a new coarse space for FETI-DP methods applied to almost incompressible linear elasticity in 3D implemented by deflation, see [11].

3 Coarse Spaces from Local Eigenvalue Problems

Let $\Omega \subset \mathbb{R}^2$, be a bounded polyhedral domain, let $\partial\Omega_D \subset \partial\Omega$ be a closed subset of positive measure, and $\partial\Omega_N := \partial\Omega \setminus \partial\Omega_D$ be its complement. We impose homogeneous Dirichlet and general Neumann boundary conditions on these two subsets, respectively, and introduce the Sobolev space $H_0^1(\Omega,\partial\Omega_D) := \{v \in H^1(\Omega) : v = 0 \text{ on } \partial\Omega_D\}$. We consider the piecewise linear conforming finite element approximation of the scalar diffusion problem:
Find $u \in H_0^1(\Omega,\partial\Omega_D)$, such that $a(u,v) = f(v) \;\; \forall v \in H_0^1(\Omega,\partial\Omega_D)$. Here, we use $a(u,v) := \int_\Omega \rho(x)\nabla u \cdot \nabla v \; dx$ and $f(v) := \int_\Omega fv \; dx + \int_{\partial\Omega_N} g_N v \; ds$, where g_N is the boundary data defined on $\partial\Omega_N$. We assume $\rho(x) > 0$ for $x \in \Omega$ and that ρ is piecewise constant on Ω. As a second model problem, we consider the problem of linear elasticity. For the compressible case we use the standard variational formulation to find a displacement $u \in (H_0^1(\Omega,\partial\Omega_D))^2$, such that $a(u,v) = f(v) \;\; \forall v \in (H_0^1(\Omega,\partial\Omega_D))^2$, where $a(u,v) := \int_\Omega G(x)\varepsilon(u) : \varepsilon(v) + G(x)\beta(x)\mathrm{div}(u)\mathrm{div}(v)dx$. The material parameters G and β will be expressed by $G = \frac{E}{1+\nu}$ and $\beta = \frac{\nu}{1-2\nu}$, using Young's modulus E and Poisson's ratio ν. The finite element space is denoted by V^h. We decompose Ω into N nonoverlapping subdomains Ω_i, $i = 1,\dots,N$, where each Ω_i is the union of shape-regular and triangular finite elements with element nodes on the boundaries of neighboring subdomains matching across the interface $\Gamma := \overline{(\cup_{i=1}^N \partial\Omega_i) \setminus \partial\Omega}$. The diameter of a subdomain Ω_i is H_i or generically $H := \max_i H_i$.

Our goal is to solve multiscale, heterogenous problems with coefficient distributions as shown in Fig. 1 efficiently using the FETI-DP or BDDC method. Here, we have highly varying coefficients inside subdomains.

In the following, we will use a new approach to obtain independence of the coefficient jumps by solving local eigenvalue problems and enriching the coarse space with eigenvectors. For other approaches, designed for certain classes of coefficients; see, e.g., [14, 22]. Similar approaches have been used for Schwarz methods in [9, 5, 4]. Another approach to create adaptive coarse spaces was introduced in [18].
Let $\mathscr{E}^{ij}$ be an edge between the subdomains Ω_i and Ω_j and let $S^{(i)}_{\mathscr{E}^{ij},\rho}$ be the Schur complement that results after eliminating all variables except of the dual displacement degrees of freedom on the edge. Let $s^{(i)}_{\mathscr{E}^{ij},\rho}(u,v) := u^T S^{(i)}_{\mathscr{E}_{ij},\rho} v$ be the corresponding bilinear form and let $m_{\mathscr{E}^{ij},\rho}(u,v) := \int_{\mathscr{E}^{ij}} \rho u \cdot v \, ds$. In the case where the Poincaré constant depends on a large jump in the coefficients, we solve the following generalized eigenvalue problem on the edge: Find $u \in V^h(\mathscr{E}^{ij})$ such that

$$s^{(i)}_{\mathscr{E}^{ij},\rho}(u,v) = \mu m_{\mathscr{E}^{ij},\rho}(u,v) \qquad \forall v \in V^h(\mathscr{E}^{ij}). \tag{1}$$

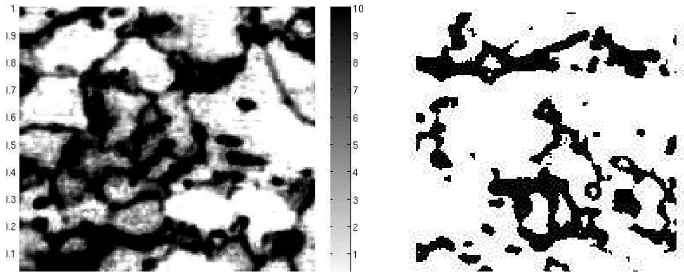

Fig. 1 Microstructures obtained from electron backscatter diffraction (EBSD/FIB). Courtesy of Prof. Dr.-Ing. Jörg Schröder, Essen, Germany, originating from a cooperation with ThyssenKrupp Steel. We have set the coefficient $E_1 = 1$ for white and $E_2 = 1e+06$ for black. An interpolated value is used for the different shades of gray. Left: gray scale image. Right: binary image. See Tab. 6 for the numerical results.

We do not need to solve this problem for all but only for the smallest eigenvalues and corresponding eigenvectors. Let the eigenvalues $0 = \mu_1 \leq \ldots \leq \mu_{n_{\mathscr{E}_{ij}}}$ be sorted in ascending order. For a given natural number $L \leq n_{\mathscr{E}_{ij}}$ and for every subdomain, we define the projection $I_L^{(l)} v := \sum_{k=1}^{L} m_{\mathscr{E}^{ij},\rho}(u_k^{(l)}, v) u_k^{(l)},\ l = i, j$, where $u_k^{(l)}$ are the eigenvectors of (1) corresponding to the eigenvalues μ_k. In our FETI-DP algorithm and the corresponding condition number estimate, we need to force the projected jumps across the interface to be zero to obtain $I_L^{(i)} v^{(i)} = I_L^{(i)} v^{(j)}$ and $I_L^{(j)} v^{(i)} = I_L^{(j)} v^{(j)}$. Let $v_{\mathscr{E}^{ij}}^{(i)}$ be the restriction of $v^{(i)}$ to the edge $\mathscr{E}^{ij}$. To guarantee this equality, we enforce the constraint $m_{\mathscr{E}^{ij},\rho}(u_k^{(l)}, v_{\mathscr{E}^{ij}}^{(i)} - v_{\mathscr{E}^{ij}}^{(j)}) = 0$ for $k = 1, \ldots, L$ and $l = i, j$. We enrich our coarse space with the eigenvectors multiplied with the mass matrix corresponding to $m_{\mathscr{E}^{ij},\rho}$ and extended by zero on the remaining part of the interface as columns of U. We do this for each subdomain, for each edge of the subdomain, and for each eigenvector of the generalized eigenvalue problem for that edge with an eigenvalue smaller than a chosen tolerance Tol_{eig}.

The next theorem is proven in [13] under certain technical assumptions.

Theorem 1. *The condition number for our FETI-DP method satisfies*

$$\kappa(\hat{M}^{-1}F) \leq C \left(1 + \log\left(\frac{\eta}{h}\right)\right)^2 \left(1 + \frac{1}{\eta \mu_{L+1}}\right),$$

where $\hat{M}^{-1} = M_{PP}^{-1}$ or $\hat{M}^{-1} = M_{BP}^{-1}$. Here, $C > 0$ is a constant independent of H, h, and η.

Next, we present numerical results for certain exemplary coefficient distributions. We use M_{BP}^{-1} choosing M^{-1} as the Dirichlet preconditioner. We subdivide the unit square into square subdomains and consider a coefficient distribution with different numbers of channels cutting through subdomain edges; see Fig. 2. We first present our results for the scalar case followed by the results for linear elasticity with discontinuous coefficients. At the end of this section, we also present our results obtained for the linear elastic deformation of the microstructures shown in Fig. 1. In our tables, we denote the FETI-DP algorithm using only vertices as primal constraints as "Algorithm A"; see [23, p. 170]. When the coarse space is enhanced using eigenvectors obtained from local eigenvalue problems the corresponding columns are denoted by "Adaptive". The additional constraints are implemented using deflation or balancing. They could also be implemented using a transformation of basis. Our stopping criterion is the relative reduction of the preconditioned residual by $1e-10$.

All experiments for the diffusion equation with heterogeneous coefficients inside subdomains are carried out with homogeneous Dirichlet boundary conditions on $\partial\Omega$ and a constant right hand side $f = 1/10$. For one channel for each subdomain, we have a quasi-monotone coefficient; cf. [21]. In this case, which is depicted in Fig. 2 (middle), on each interior edge, the eigenvector of the eigenvalue zero is added to the coarse space. On interior edges which do not intersect a channel with a high coefficient the resulting constraint is a standard edge average. On interior edges intersected by a channel the constraint is a weighted edge average, cf. also [14], up to a multiplicative constant. This results in eight adaptive constraints; see Tab. 1. The case of three channels results in 20 adaptive constraints.

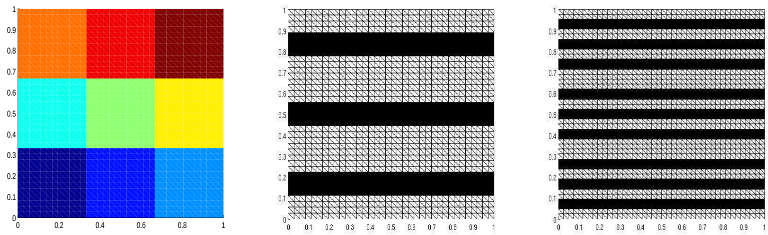

Fig. 2 Domain decomposition in nine subdomains (left). The coefficient distribution is depicted for one channel (middle) and three channels (right). Here, black corresponds to a high coefficient and white corresponds to $\rho = 1$ (middle/right).

In Tab. 2, for three channels, we see that the condition number using the enriched coarse space stays bounded if we change the contrast $\rho_2 \in \{1, \ldots, 1e+06\}$. Moreover, the number of adaptive constraints approaches a limit for growing contrast.

In Tab. 3 we see that for an increasing number of subdomains and channels the condition number remains bounded. The number of adaptive constraints grows roughly in proportion to the number of subdomains and channels. Note that the adaptive algorithm with $Tol_{\text{eig}} = 1$ chooses only constraints on subdomains, where the Dirichlet boundary does not intersect the inclusions. On subdomains with Dirichlet boundary conditions that do not intersect the channels, six constraints, and on all inner subdomains, 8 constraints are chosen. Linearly dependent constraints are detected using the modified Gram-Schmidt method and removed.

Next, we test our algorithm on linear elasticity problems with certain distributions of varying coefficients inside subdomains. We impose homogeneous Dirichlet

# Channels	H/h	Algorithm A condition	Algorithm A # its	**Adaptive Method** condition	**Adaptive Method** # its	# Adaptive constraints	Size of Γ
1	6	$9.5532e+04$	7	**1.0412**	**3**	8	84
	12	$1.1969e+05$	7	**1.1547**	**4**	8	156
	18	$1.3335e+05$	7	**1.2519**	**4**	8	228
	24	$1.4416e+05$	8	**1.3325**	**4**	8	300
	30	$1.5197e+05$	8	**1.4011**	**5**	8	372
3	14	39.2087	6	**1.0387**	**2**	20	180
	28	$1.3431e+05$	10	**1.1507**	**3**	20	348
	42	$1.3884e+05$	11	**1.2471**	**3**	20	516
	56	$1.8408e+05$	14	**1.3272**	**3**	20	684
	70	$1.9298e+05$	13	**1.3954**	**3**	20	852

Table 1 Scalar diffusion, one and three channels for each subdomain, see Fig. 2 (right). We have $\rho = 1e+06$ in the channel, and $\rho = 1$ elsewhere. The number of additional constraints is clearly determined by the structure of the heterogeneity and independent of the mesh size. $1/H = 3$. Tol_{eig}=1.

ρ_2/ρ_1	Algorithm A condition	Algorithm A # its	**Adaptive Method** condition	**Adaptive Method** # its	# Adaptive constraints	Size of Γ
1	3.2068	5	**1.6467**	**5**	4	348
10	5.5781	7	**1.5697**	**7**	4	348
$1e+02$	19.9519	9	**1.4604**	**7**	8	348
$1e+03$	$1.5891e+02$	9	**1.1506**	**4**	20	348
$1e+04$	$1.5476e+03$	11	**1.1507**	**3**	20	348
$1e+05$	$1.5434e+04$	12	**1.1507**	**3**	20	348
$1e+06$	$1.3431e+05$	10	**1.1507**	**3**	20	348

Table 2 Scalar diffusion, three channels for each subdomain, see Fig. 2 (right). We have $\rho = \rho_2$ in the channels, and $\rho = \rho_1 = 1$ elsewhere. $H/h = 28$. The number of additional constraints is bounded for increasing contrast ρ_2/ρ_1. $1/H = 3$. Tol_{eig}=1.

$1/H$	Algorithm A condition	Algorithm A # its	**Adaptive Method** condition	**Adaptive Method** # its	# Adaptive constraints	Size of Γ
2	1.1507	4	**1.1507**	**4**	0	114
3	$1.3431e+05$	10	**1.1507**	**3**	20	348
4	$2.3766e+05$	16	**1.1507**	**3**	44	702
5	$3.0209e+05$	45	**1.1507**	**3**	78	1176
6	$3.5451e+05$	51	**1.1507**	**3**	122	1770

Table 3 Scalar diffusion, three channels for each subdomain; see Fig. 2 (right). Increasing number of subdomains and channels. We have $\rho = 1e+06$ in the channel, and $\rho = 1$ elsewhere. $H/h = 28$. Tol_{eig}=1.

boundary conditions only on the lower edge, i.e., $y = 0$, and a constant volume force $f = (1/10, 1/10)^T$. First we consider the example above with three channels and with jumps in E instead of ρ. Tab. 4 and 5 show the numerical results for a tolerance of one for the eigenvalues. Finally, we use a coefficient distribution obtained from a steel microsection pattern with 150×150 pixels; see Fig. 1. We discretize the problem with $H/h = 50$ and $1/H = 3$; see Tab. 6 for the numerical results, which show the effectiveness of the adaptive algorithm.

		Algorithm A		**Adaptive Method**		# Adaptive	Size of
# Channels	H/h	condition	# its	condition	# its	constraints	Γ
3	14	$6.8833e+05$	335	**1.1517**	**8**	123	372
	28	$9.3377e+05$	348	**1.3351**	**10**	123	708
	42	$1.0821e+06$	347	**1.4993**	**10**	123	1044

Table 4 Linear elasticity, three channels for each subdomain, see Fig. 2, with coefficient $E = 1e+06$, outside the channels $E = 1$. $Tol_{\text{eig}} = 1$. The number of additional constraints is determined by the structure of the heterogeneity and independent of the mesh size; $1/H = 3$.

	Algorithm A		**Adaptive Method**		# Adaptive	Size of
E_2/E_1	condition	# its	condition	# its	constraints	Γ
1	6.2497	22	**1.9264**	**12**	33	708
10	15.7940	27	**1.8460**	**12**	34	708
$1e+02$	$1.0256e+02$	39	**1.9836**	**13**	65	708
$1e+03$	$9.4413e+02$	61	**1.3398**	**9**	90	708
$1e+04$	$9.3490e+03$	117	**1.3363**	**9**	99	708
$1e+05$	$9.3373e+04$	191	**1.3352**	**9**	111	708
$1e+06$	$9.3377e+05$	348	**1.3351**	**10**	123	708

Table 5 Linear elasticity, three channels for each subdomain, see Fig. 2, $H/h = 28$. The number of additional constraints is bounded for increasing contrast E_2/E_1. $1/H = 3$, Tol_{eig}=1.

Problem	Coarse space	H/h	condition	# its	# Adaptive constraints	Size of Γ
Fig. 1 (left)	Adaptive	50	**21.6171**	**24**	114	1236
	Algorithm A	50	$> 3e+05$	> 250	0	1236
Fig. 1 (right)	Adaptive	50	**10.2617**	**22**	114	1236
	Algorithm A	50	$> 1e+06$	> 250	0	1236

Table 6 Results for linear elasticity using the coefficient distribution for the heterogenous problem from the gray scale image in Fig. 1.

4 Domain decomposition methods for nonlinear problems

The traditional domain decomposition approach to nonlinear problems can be characterized by a geometric decomposition after linearization. Here, we solve a given nonlinear, discretized problem

$$A(u) = 0 \tag{2}$$

by using a Newton-type method $u^{(k+1)} = u^{(k)} - \alpha^{(k)} \delta u^{(k)}$ with a suitable step length $\alpha^{(k)}$. In each iteration we have to solve the linearized system $DA(u^{(k)})\delta u^{(k)} = A(u^{(k)})$ which can be done by overlapping or nonoverlaping domain decomposition methods, e.g., FETI-1, FETI-DP, BDDC, or overlapping Schwarz. Such approaches are typically named NK-DD (Newton-Krylov-Domain-Decomposition), i.e., NK-FETI-DP, NK-Schwarz, etc.

Alternative approaches to the traditional DD approach can be characterized by linearization after a geometric decomposition (here denoted as DD-NK, i.e., FETI-DP-NK). Such methods can be interpreted also in the context of nonlinear preconditioning, as, e.g., performed in the ASPIN approach, see [2], which can be viewed as solving a nonlinear equation $G(A(u)) = 0$ by a Newton method instead of (2). The nonlinear preconditioner G is constructed from a nonlinear additive Schwarz (AS) method. The ASPIN approach can be classified as an AS-NK method and has been shown to be more robust and highly scalable, e.g., even for high Reynolds flow problems. Recently, the ASPIN approach has successfully been applied in nonlinear structural mechanics [12].

In this paper, we will present new approaches for nonoverlapping, nonlinear DD methods, i.e., versions of nonlinear FETI-DP methods. We will discuss two different strategies of nonlinear dual primal FETI methods, named Nonlinear-FETI-DP-1 (Linearization first) and Nonlinear-FETI-DP-2 (Elimination first).

Nonlinear, nonoverlapping domain decomposition methods have been used, in the special case of two subdomains, in multiphysics coupling, e.g., in fluid-structrure interaction; see [3]. Recently, a nonlinear FETI domain decomposition approach for nonlinear problems from elasticity was suggested by Pebrel, Rey, and Gosselet [20]. A simple linear/nonlinear strategy was used in [16] for brittle materials with strongly localized nonlinearities.

Let $\Omega_i, i = 1,\dots,N$, be a decomposition of our domain Ω into nonoverlapping subdomains. We denote the associated local finite element spaces by W_i and the product space by $W = W_1 \times \dots \times W_N$. We define $\widehat{W} \subset W$ as the subspace of functions from W which are continuous in all interface variables between subdomains. We consider the minimization of a global nonlinear energy function $\widehat{J}$, operating on $\widehat{W}$,

$$\hat{u} = \arg\min_{\hat{v} \in \widehat{W}} \widehat{J}(\hat{v}).$$

Using our decomposition of Ω we can build local nonlinear energy functions $J_i, i = 1,\dots,N$, operating on W_i, and equivalently solve

$$u = \arg\min_{v \in W} \textstyle\sum_{i=1}^{N} J_i(v_i)$$

under the linear continuity constraint $Bu = 0$. Here, B is a linear jump operator, which enforces continuity in all interface variables. At this point using a variational formulation and standard dualization technique, leads us to a nonlinear saddle point problem

$$\begin{aligned} K(u) + B^T\lambda &= f \\ Bu &= 0, \end{aligned}$$

where $K(u)^T := (K_1(u_1)^T, \ldots, K_N(u_N)^T)$ and $f^T := (f_1^T, \ldots, f_N^T)$.

Using the standard FETI-DP operator R_Π^T, see [14] for the notation, to perform the partial assembly in the primal variables, we formulate the nonlinear FETI-DP master system

$$\begin{aligned} R_\Pi^T K(R_\Pi \tilde{u}) + B^T\lambda - \tilde{f} &= 0 \\ B\tilde{u} &= 0, \end{aligned} \tag{3}$$

where $\tilde{f} := R_\Pi^T f$, $\tilde{u} \in \widetilde{W}$, and the Lagrange multipliers $\lambda \in V$. Here, B enforces continuity in the dual unknowns. We can proceed in two different ways in order to solve (3). We may linearize first and then reduce the result to Lagrange multipliers (Nonlinear-FETI-DP-1), or, using the implicit function theorem, we can use nonlinear elimination and then linearization of the reduced nonlinear system (Nonlinear-FETI-DP-NK-2).

We now consider the first approach *Nonlinear-FETI-DP-1* (Linearize first). With given initial values $\tilde{u}^{(0)} \in \widetilde{W}$ and $\lambda^{(0)} \in V$, we can formulate the following Newton iteration to solve problem (3),

$$\begin{pmatrix} \tilde{u}^{(k+1)} \\ \lambda^{(k+1)} \end{pmatrix} = \begin{pmatrix} \tilde{u}^{(k)} \\ \lambda^{(k)} \end{pmatrix} - \alpha^{(k)} \begin{pmatrix} \delta\tilde{u}^{(k)} \\ \delta\lambda^{(k)} \end{pmatrix},$$

with a suitable step length $\alpha^{(k)}$. In each iteration we need to solve

$$\begin{pmatrix} R_\Pi^T DK(R_\Pi \tilde{u}^{(k)}) R_\Pi & B^T \\ B & 0 \end{pmatrix} \begin{pmatrix} \delta\tilde{u}^{(k)} \\ \delta\lambda^{(k)} \end{pmatrix} = \begin{pmatrix} R_\Pi^T K(R_\Pi \tilde{u}^{(k)}) + B^T\lambda^{(k)} - \tilde{f} \\ B\tilde{u}^{(k)} \end{pmatrix}. \tag{4}$$

This system can be treated as in a standard FETI-DP framework, i.e., we can reduce (4) to the Lagrange multipliers. The difference to the standard NK-FETI-DP iteration can be found on the right hand side of (4). Note that, as a result of $B\delta\tilde{u}^{(k)} = B\tilde{u}^{(k)}$, jumps in the Newton update will be present only if the initial value has jumps.

In this paper, we have choosen the initial value $\lambda^{(0)} = 0$ and computed the initial value $\tilde{u}^{(0)}$ by solving the nonlinear problem

$$R_\Pi^T K(R_\Pi \tilde{u}^{(0)}) + B^T\lambda^{(0)} - \tilde{f} = 0,$$

by some Newton-type iteration. Note, that here we solve local nonlinear subdomain problems which are only coupled in the primal unknows.

Let us now consider the second approach *Nonlinear-FETI-DP-2* (Eliminate first). Instead of linearizing the nonlinear saddle point problem (3), we may perform a nonlinear elimination of the variable $\tilde{u}$ first. To simplify our notation, let us define the nonlinear operator

$$\widetilde{K}(\tilde{u}) = R_{\Pi}^T K(R_{\Pi}\tilde{u}).$$

Under sufficient assumptions the first equation of (3) can be written as

$$\tilde{u} = \widetilde{K}^{-1}(\tilde{f} - B^T\lambda), \tag{5}$$

where $\widetilde{K}^{-1}$ is the inverse map of $\widetilde{K}$. Inserting (5) into the continuity condition in (3) we obtain

$$F(\lambda) = B\widetilde{K}^{-1}(\tilde{f} - B^T\lambda) = 0. \tag{6}$$

Again we use a Newton-type iteration to solve (6), and obtain the iteration

$$\lambda^{(k+1)} = \lambda^{(k)} - \alpha^{(k)}(D_\lambda F(\lambda^{(k)}))^{-1}F(\lambda^{(k)}).$$

We can compute $D_\lambda F(\lambda)$ using the chain rule, the inverse function theorem, and (5),

$$\begin{aligned} D_\lambda F(\lambda) &= D_\lambda(B\widetilde{K}^{-1}(\tilde{f} - B^T\lambda)) = -B(D\widetilde{K}^{-1}(\tilde{f} - B^T\lambda))B^T \\ &= -B(D\widetilde{K}(\tilde{u}))^{-1}B^T = -B(R_{\Pi}^T(DK(R_{\Pi}\tilde{u})R_{\Pi})^{-1}B^T. \end{aligned}$$

In each Newton step, we have to solve a nonlinear system with a FETI-DP-type matrix on the left hand side and $F(\lambda^{(k)}) = B\widetilde{K}^{-1}(\tilde{f} - B^T\lambda^{(k)})$ on the right hand side. On the right hand side nonlinear local problems have to be solved which are only coupled in the primal variables.

In contrast to a standard Newton-Krylov-FETI-DP approach, in our nonlinear FETI-DP methods weakly coupled nonlinear local problems are solved. We expect to reduce communication and to obtain a significantly improved performance especially for problems with localized nonlinearities.

Next, we introduce our nonlinear model problem and present numerical results for our two nonlinear FETI-DP approaches. Let us define the p-Laplacian for $p = 4$ as

$$\Delta_4 v = \mathrm{div}(|\nabla v|^2 \nabla v).$$

We test our algorithms for nonlinear model problems with and without localized nonlinearities. For our experiments, we consider the unit square $\Omega := [0,1] \times [0,1]$ in 2D decomposed into square subdomains $\Omega_i, i = 1,\ldots,N$. We have chosen piecewise linear triangular elements to discretize the variational formulations of (7) and (8).

First we solve the following equation for the p-Laplacian with $p = 4$ on the complete domain, i.e.,

$$\begin{aligned} \Delta_4 u &= -1 \qquad \text{in } \Omega \\ u &= \ \ 0 \qquad \text{on } \partial\Omega. \end{aligned} \tag{7}$$

In our second set of numerical experiments we consider the (linear) Laplace equation with nonlinear inclusions inside subdomains; see Fig. 3. The inclusions are surrounded by hulls of width η. This configuration can be seen as a nonlinear analog to the problem of [10]. We denote the hull on subdomain Ω_i by $\Omega_{i,\eta}$

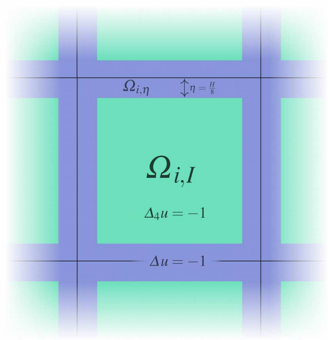

Fig. 3 Domain Ω_i with an inclusion $\Omega_{i,I}$ and $\eta = \frac{H}{8}$.

and the inclusion by $\Omega_{i,I} = \Omega_i \setminus \Omega_{i,\eta}$. Furthermore we define $\Omega_I = \bigcup_{i=1}^N \Omega_{i,I}$ and $\Omega_\eta = \bigcup_{i=1}^N \Omega_{i,\eta}$.

We then solve

$$\begin{aligned} \Delta_4 u &= -1 && \text{in } \Omega_I \\ \Delta u &= -1 && \text{in } \Omega_\eta \\ u &= 0 && \text{on } \partial\Omega. \end{aligned} \tag{8}$$

In our tests all vertices are primal and, additionally, we use primal edge constraints in our linear and nonlinear FETI-DP methods. We compare the traditional NK-FETI-DP with our nonlinear FETI-DP variants. To perform a fair comparison of the computational cost, we consider the number of Krylov space iterations and the number of linearizations separately. Each linearization includes the assembly of the local tangential matrices and their LU-decomposition. The results for problems (7) and (8) can be found in Tab. 7. The computational costs for the new methods are significantly lower for both problems, especially for the problem with local nonlinearities (p-Laplace inclusions). The number of global Krylov iterations is reduced radically and therefore, in a parallel setting, also communication.

5 Conclusion

We have presented an approach for the construction of an adaptive coarse space in FETI-DP algorithms by computing certain generalized eigenvalue problems. The method is motivated directly from the theory, i.e., a Poincaré inequality needed in the condition number estimate is now replaced by a computational bound.

		p-Laplace inclusions				p-Laplace			
N	**Solver**	**# Krylov It.**	**# Lin.**	**max. cond.**	**min. cond.**	**# Krylov It.**	**# Lin.**	**max. cond.**	**min. cond.**
4	NK-FETI-DP	33	14	1.0048	1.0001	72	18	1.1352	1.0608
	Nonlinear-FETI-DP-2	5	14	1.2813	1.0000	8	19	1.0644	1.0604
	Nonlinear-FETI-DP-1	5	15	1.2805	1.0001	12	20	1.0644	1.0604
16	NK-FETI-DP	105	15	1.4719	1.2914	164	20	1.4605	1.4107
	Nonlinear-FETI-DP-2	21	18	1.4240	1.4233	32	29	1.4208	1.4012
	Nonlinear-FETI-DP-1	28	18	1.4240	1.4233	40	24	1.4208	1.4108
64	NK-FETI-DP	164	17	1.5680	1.4264	226	22	1.5302	1.4895
	Nonlinear-FETI-DP-2	30	20	1.5255	1.5197	52	33	2.1258	1.4878
	Nonlinear-FETI-DP-1	40	20	1.5254	1.5197	52	26	2.1258	1.4850
256	NK-FETI-DP	190	19	1.5852	1.5281	268	24	1.6846	1.5394
	Nonlinear-FETI-DP-2	31	22	1.5643	1.5412	44	34	2.1523	1.5237
	Nonlinear-FETI-DP-1	42	22	1.5654	1.5406	55	28	2.1523	1.5375
1024	NK-FETI-DP	209	21	1.5786	1.4939	293	26	1.9809	1.5642
	Nonlinear-FETI-DP-2	31	24	1.5827	1.5409	45	35	2.1669	1.4921
	Nonlinear-FETI-DP-1	43	24	1.5852	1.5409	56	30	2.1669	1.5560
4096	NK-FETI-DP	215	23	1.5784	1.4972	330	28	2.5309	1.5657
	Nonlinear-FETI-DP-2	19	25	1.5768	1.5451	45	37	2.1743	1.4890
	Nonlinear-FETI-DP-1	41	26	1.5938	1.5451	45	31	2.1743	1.5588

Table 7 *p-Laplace* is described in (7) and *p-Laplace inclusions* is described in (8). For *p-Laplace inclusions*, see also Fig. 3. In both problems, $\frac{H}{h} = 16$; N is the number of subdomains; *# Krylov It.* gives the sum of all Krylov-space iterations; *# Lin.* gives the sum of all linearizations (computing local tangential matrices and their LU-decomposition); *min./max. cond* give the maximal and minimal condition number of the FETI-DP systems.

We have also presented approaches to construct nonlinear versions of the FETI-DP method. In these methods, the coarse space takes an important role since it can influence not only the convergence of the Krylov method but also that of the Newton iteration. In the future, the use of an adaptive coarse space may therefore be of special interest in this context.

Acknowledgements This work was supported (in part) by the German Research Foundation (DFG) through the Priority Programme 1648 ”Software for Exascale Computing” (SPPEXA).

References

1. Dohrmann, C., *A preconditioner for substructuring based on constrained energy minimization*, SIAM J. Sci. Comput., 25 (2003), pp. 246–258.
2. Cai, X.C., Keyes, D.E.: Nonlinearly preconditioned inexact Newton algorithms. SIAM J. Sci. Comput. **24**(1), 183–200 (electronic) (2002). DOI 10.1137/S106482750037620X
3. Deparis, S., Discacciati, M., Fourestey, G., Quarteroni, A.: Fluid-structure algorithms based on Steklov-Poincaré operators. Comput. Methods Appl. Mech. Engrg. **195**(41-43), 5797–5812 (2006). DOI 10.1016/j.cma.2005.09.029
4. Dolean, V., Hauret, P., Nataf, F., Pechstein, C., Scheichl, R., Spillane, N.: Abstract Robust Coarse Spaces for Systems of PDEs via Generalized Eigenproblems in the Overlaps. NuMa-

Report, Institute of Computational Mathematics, Johannes Kepler University Linz **7** (2011)
5. Dolean, V., Nataf, F., Scheichl, R., Spillane, N.: Analysis of a two-level Schwarz method with coarse spaces based on local Dirichlet-to-Neumann maps. http://hal.archives-ouvertes.fr/docs/00/58/62/46/PDF/paper14avril.pdf (2011)
6. Dostál, Z., *Conjugate gradient method with preconditioning by projector*, Intern. J. Computer Math. **23** (1988), 315–323.
7. Dryja, M. and Widlund, O. B., *Schwarz methods of Neumann-Neumann type for three-dimensional elliptic finite element problems*, Comm. Pure Appl. Math., **48**:2 (1995), 121–155.
8. Farhat, C., Lesoinne, M., LeTallec, P., Pierson, K., and Rixen, D., *FETI-DP: A dual-primal unified FETI method - part i: A faster alternative to the two-level FETI method*, Internat. J. Numer. Methods Engrg., **50** (2001), 1523–1544.
9. Galvis, J., Efendiev, Y.: Domain decomposition preconditioners for multiscale flows in high contrast media: reduced dimension coarse spaces. Multiscale Model. Simul. **8**(5), 1621–1644 (2010). DOI 10.1137/100790112
10. Gippert, S., Klawonn, A., Rheinbach, O.: Analysis of FETI-DP and BDDC for linear elasticity in 3D with almost incompressible components and varying coefficients inside subdomains. SIAM J. Numer. Anal. **50**(5), 2208–2236 (2012)
11. Gippert, S., Klawonn, A., Rheinbach, O.: A Deflation Based Coarse Space in Dual-Primal FETI Methods for Almost Incompressible Elasticity Submitted to the Proceedings of the European Conference on Numerical Mathematics and Advanced Applications (ENUMATH), Lausanne, August 26-30, 2013. Springer Lecture Notes in Comput. Sci. Engrg., 8p.
12. Groß, C., Krause, R.: On the globalization of ASPIN employing trust-region control strategies - convergence analysis and numerical examples. Tech. Rep. 2011-03, Institute of Computational Science, Universita della Svizzera italiana (2011)
13. Klawonn, A., Radtke, P., Rheinbach, O.: FETI-DP methods with an adaptive coarse space. Preprint (2013), submitted for publication.
14. Klawonn, A., Rheinbach, O.: Robust FETI-DP methods for heterogeneous three dimensional elasticity problems. Comput. Methods Appl. Mech. Engrg. **196**(8), 1400–1414 (2007). DOI 10.1016/j.cma.2006.03.023
15. Klawonn, A., Rheinbach, O.: Deflation, projector preconditioning, and balancing in iterative substructuring methods: connections and new results. SIAM J. Sci. Comput. **34**(1), A459–A484 (2012). DOI 10.1137/100811118
16. Lloberas-Valls, O., Rixen, D.J., Simone, A., Sluys, L.J.: Domain decomposition techniques for the efficient modeling of brittle heterogeneous materials. Comput. Methods Appl. Mech. Engrg. **200**(13-16), 1577–1590 (2011). DOI 10.1016/j.cma.2011.01.008
17. Mandel, J., *Balancing domain decomposition*, Comm. Numer. Meth. Engrg. **9** (1993), 233–241.
18. Mandel, J., Sousedík, B.: Adaptive coarse space selection in the BDDC and the FETI-DP iterative substructuring methods: optimal face degrees of freedom. In: Domain decomposition methods in science and engineering XVI, *Lect. Notes Comput. Sci. Eng.*, vol. 55, pp. 421–428. Springer, Berlin (2007). DOI 10.1007/978-3-540-34469-8_52. URL `http://dx.doi.org/10.1007/978-3-540-34469-8_52`
19. Nicolaides, R. A., *Deflation of conjugate gradients with applications to boundary value problems*, SIAM J. Numer. Anal., **24:2** (1987), 355–365.
20. Pebrel, J., Rey, C., Gosselet, P.: A nonlinear dual-domain decomposition method: Application to structural problems with damage. Inter. J. Multiscal Comp. Eng. **6**(3), 251–262 (2008)
21. Pechstein, C., Scheichl, R.: Weighted Poincaré inequalities. NuMa-Report, Institute of Computational Mathematics, Johannes Kepler University Linz **10** (2010)
22. Pechstein, C., Scheichl, R.: Analysis of FETI methods for multiscale PDEs. Part II: interface variation. Numer. Math. **118**(3), 485–529 (2011). DOI 10.1007/s00211-011-0359-2
23. Toselli, A. and Widlund, O. B., *Domain decomposition methods-algorithms and theory*, vol. 34, Springer, 2004.